CHAPTER 2

VARIATION AND RELATIONSHIP OF PM2.5, AOD 550 nm AND METEOROLOGICAL PARAMETERS OVER BRAHMAPUTRA VALLEY AT THE VALLEY-SITE SCALE

2.1 INTRODUCTION

PM2.5 are microscopic aerosol particles smaller than 2.5μm in aerodynamic diameter responsible for poor air quality [1]. PM2.5 have high potential for causing adverse health problems such as premature mortality, allergic reactions, lung dysfunction, respiratory and cardiovascular diseases [2-5]. The Aerosol Optical Depth (AOD) is the key parameter for measuring the columnar aerosol load. It represents the integral of the total extinction (scattering and absorption) of solar light by aerosols in the atmospheric column [6]. Both the parameters, therefore, are widely used by the scientific community for aerosol studies.

Variations in PM2.5 surface concentration, AOD 550 nm and meteorological forcing parameters are common occurrences over a large geographical area. The magnitude and heterogeneity of variation vary widely over space, seasons and topography. Aerosol variability over space and time is largely governed by meteorological forcing variables- AT, WS, RH, Ps- through several mechanisms (discussed in Table 2.1) over a region. The other factors that impact the aerosol variability are large-scale high and low pressure systems, diurnal heating and cooling cycle, boundary layer dynamism, local wind pattern, and available moisture.

The topographical orientation and terrain complexity of BV play an important role in local meteorological conditions and the accumulation of aerosols over the valley. The complex terrain of BV strongly influences the local wind circulations (upslope and downslope flow of wind due to terrain contrast), horizontal advection and terrain induced flow modification. The continental and biogenic aerosols sourced from the vegetation, carbonaceous aerosols emitted from fossil and biofuel combustion, and the long-range transported sea salt and dust particles from the BoB, IGP and west Asia along with the micro-meteorological conditions have a cumulative effect on the accumulation of aerosols within the valley [7-10]. The aerosol loading is further magnified by the presence of uplifted aerosol plumes in the atmosphere over the eastern Himalayas [11,12].

Table 2.1 A review of the mechanism between PM2.5 surface concentration and different meteorological parameters.

Parameter	Feedback mechanism	Reference
WS and PM2.5	PM2.5 is highly sensitive to speed and direction of near-surface winds as they determine their mean transport speed and direction once released from near-ground sources	Arya 1999 [13]
RH and PM2.5	High humidity in the atmosphere increases the aqueous uptake of semi-volatile materials (such as nitrate and organic aerosol), thus enhancing their hygroscopic growth	Koch et al. 2003; Wise and Comrie 2005 [14, 15]
RH and PM2.5	Changes in RH can also affect the size distribution and optical properties (by modifying scattering efficiencies) of aerosol particles	Wang and Martin 2007 [16]
AT and PM2.5	AT can intensify PM2.5 photochemical reactions and the formation of particulate matter	Gupta et al. 2009; Pateraki et al. 2012 [17, 18]
WS and PM2.5	PM2.5 is inversely sensitive to wind speed, as decreases in horizontal advection can build up PM2.5 concentration	Jacob and Winner 2009; Porter et al. 2015 [19, 20]
AT and PM2.5	Warmer AT is favorable for an increase in PM2.5 production by oxidation of sulphur dioxide (SO_2) to sulfate (SO_4) aerosol whereas less advantageous for condensation of semi-volatile materials to the aerosol phase	Westervelt et al. 2016 [21]
Ps and PM2.5	High-pressure systems can lead to stable atmospheric conditions (vice-versa) and shallow mixing layer height, resulting in poor ventilation and an increase (or decrease) in PM2.5	Westervelt et al. 2016 [21]

AT= Air temperature, RH= relative humidity, WS= wind speed, Ps= surface pressure.

A comprehensive survey of the research literature on aerosol studies covering BV and the surrounding region is presented in Table 2.2. Most of the aerosol studies over BV focused on chemical characterization, source inventory, the radiative impact of aerosols, and

physical characteristics of different PM (PM2.5 and PM10) fractions mostly on select point sample sites. Despite the importance, a comprehensive analysis of spatio-temporal variation of PM2.5, AOD 550 nm and meteorological parameters at the valley-site scale over BV is rarely studied. Similarly, there is a dearth of studies understanding the relationship between PM2.5 and meteorological variables AT, RH, WS and Ps as well as with AOD 550 nm over BV.

For a fuller analysis of spatio-temporal variation in PM2.5, AOD 550 nm and meteorological parameters at the valley-site scale, a continuous spatial and temporal dataset of the parameters is an essential requirement. The inadequate number and disproportionate distribution of ground-based stations for PM2.5, AOD 550 nm and meteorological parameters, has always been a major limiting factor. Similarly, the availability and accessibility of data for a longer period is another major concern. Research worldwide shows that this limitation can be addressed by integrating satellite, reanalysis and ground-based data.

MERRA-2 is the first long-term global reanalysis tool that incorporates aerosol observations into a global assimilation system [22]. PM2.5 calculated from MERRA-2 aerosol component has well represented surface PM2.5 concentration for India [23]. Similarly, ERA5 ECMWF reanalysis meteorological products provide accurate information of land estimates at higher spatial and temporal resolutions. MODIS AOD retrievals are widely utilized for aerosol study globally.

This chapter, therefore, (a) evaluates PM2.5 surface concentration based on MERRA-2 aerosol components; (b) analyses the spatial, seasonal and inter-annual variation of PM2.5, AOD 550 nm and meteorological parameters viz. AT, WS, Ps and RH; (c) examines the nature and strength of the relationship between PM2.5 and AOD 550 nm, PM2.5 and meteorological parameters for the period 2016 to 2020.

The limitation in ground-based data, as mentioned earlier, is a hurdle in aerosol studies over BV. This chapter used MODIS onboard Terra and Aqua AOD retrievals, MERRA-2 aerosol components, and ERA ECMWF meteorological reanalysis data. Performance assessment of ERA5 meteorological data and MERRA-2 PM2.5 estimates with respect to ground-based observations are part of the scope of this chapter.

Table 2.2 A survey of the literature on aerosol studies over Brahmaputra valley.

Parameter and study area	Key conclusion/ remarks	Reference
Near-real-time measurements of the mass size distribution of composite aerosols at Dibrugarh	Accumulation mode aerosols contributed more than 50% of the total aerosol mass concentration throughout the year, west Asian locations and that over the Indo-Gangetic Plains significantly contribute to the total aerosol abundance.	Gogoi et al. 2011 [7]
BC mass concentration at Guwahati	Daily median values of BC mass concentration were 9–41 mg/m^3, with maxima over 50 mg/m^3 during evenings and early mornings.	Chakrabarty et al. 2012 [24]
AOD, water vapor, cloud fraction, cloud top temperature, cloud top pressure and cloud optical depth in Northeastern India	The highest annual mean increase of AOD (> 79%) has been found over Guwahati. AOD was found to be increased by >20 % during the last decade over Northeastern India	Kumar 2013 [25]
PM, PM10, PM2.5, BC concentration at 13 locations across BV	Spatial heterogeneity in aerosol distribution, a gradual decrease in BC concentrations from west to east of the Brahmaputra valley.	Pathak et al. 2014 [8]
Spectral aerosol optical depth, Angstrom wavelength exponent at Shillong, Agartala, Imphal and Dibrugarh	Aerosol distribution and climatic impacts show west to east gradient within the North-eastern region, the highest ARF in the atmosphere occurs in the pre-monsoon season.	Pathak et al. 2016 [26]

TOA earth radiation, AOD 550 nm; Nine locations in Northeast India	AOD over the Northeast India region with complex terrain shows altitudinal variation with maximum value at the lowest elevation site Dhaka and minimum value at the high-altitude locations, strong seasonality in AOD.	Biswas et al. 2017 [27]
PM2.5 and PM10 ground-based data at Guwahati	The local emissions, transported aerosols, along with seasonally changing air masses, meteorology and boundary-layer dynamics control the concentrations, evolution and fractions of PM over BV.	Tiwari et al. 2017 [9]
PM10 at Tezpur	Anthropogenic contributions of aerosol, particularly from biomass burning, vehicular emission, and road dust.	Bhuyan et al. 2018 [10]
BC mass concentration at Guwahati	Vehicular emission contributed over 85% of the ambient black carbon over BV. black carbon particulates are being transported and deposited all-round the year in the Himalayas and the surrounding region.	Barman and Gokhale 2019 [28]

BC= black carbon, PM= particulate matter, TOA= top-of-atmosphere, AOD=Aerosol Optical Depth, ARF= aerosol radiative forcing

2.2 DATA, SOURCES AND PRE-PROCESSING

The technical specifications along with the sources of the datasets used for the present work are given in Table 2.3. The salient features of the datasets are discussed in the following sub-sections. The ground-based stations for meteorological parameters- Guwahati, Lakhimpur and Dibrugarh, and for PM2.5 surface concentration- Tezpur over BV is shown Figure 2.1.

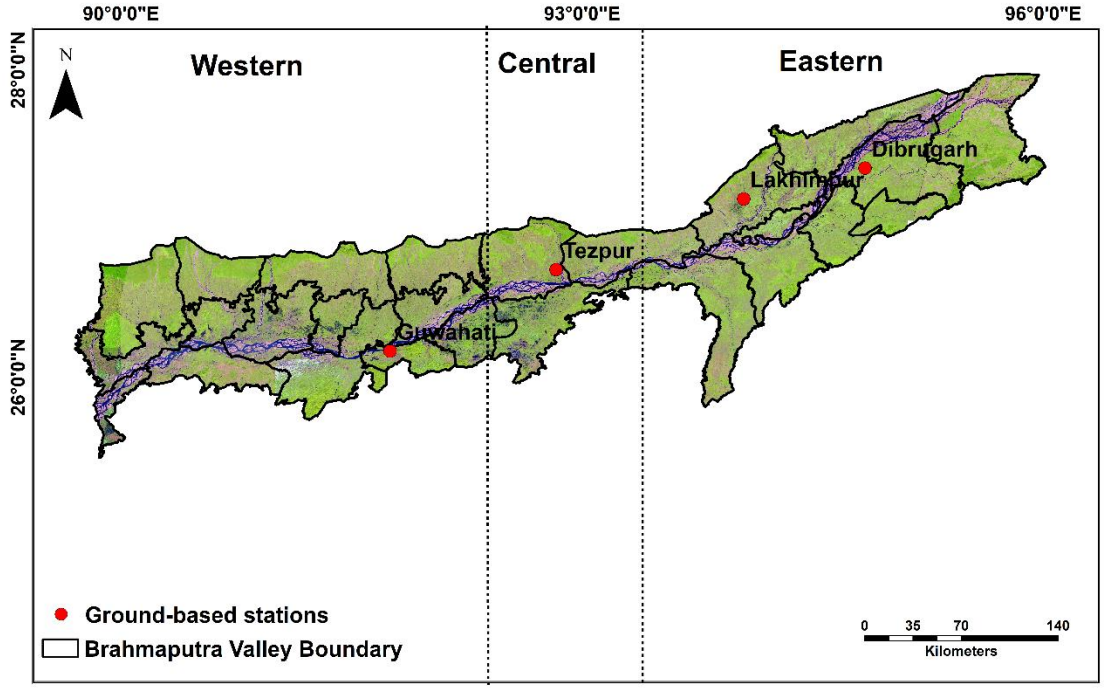

Figure 2.1 Locations of the ground-based stations for meteorological parameters and PM2.5 surface concentration over Brahmaputra Valley (for meteorological parameters- Guwahati, Lakhimpur and Dibrugarh; for PM2.5 surface concentration- Tezpur).

Table 2.3 Technical specifications and the sources of the datasets used.

Parameter	Spatial resolution	Temporal resolution	Data source	Available at
AOD 550 nm	10x10 km (native)	daily	MODIS Terra and Aqua	https://ladsweb.modaps.eosdis.nasa.gov/search/
AOD 550 nm	point	hourly	AERONET	https://aeronet.gsfc.nasa.gov/
Aerosol components - SO_4, BC, $DU_{2.5}$, $SS_{2.5}$, OC	0.5º x 0.625º (native)	hourly	MERRA-2	https://disc.gsfc.nasa.gov/
PM2.5	point	hourly	MAPAN	MAPAN Tezpur University
u and v component of wind	0.25º x 0.25º (native)	hourly	ERA5 ECMWF	https://www.ecmwf.int/en/forecasts/datasets/browse-reanalysis-datasets
AT, Ps, RH	0.25º x 0.25º (native)	hourly	ERA5 ECMWF	https://www.ecmwf.int/en/forecasts/datasets/browse-reanalysis-datasets
AT, Ps, RH, WS	point	3-hourly	IMD	https://www.imdpune.gov.in/

AT=Air temperature, Ps= Surface Pressure, RH= Relative humidity, WS= Wind speed, SO_4= Sulfate, BC= Black carbon $DU_{2.5}$= Dust, $SS_{2.5}$= Sea salt, OC= Organic carbon

2.2.1 MODIS AOD 550 nm

AOD 550 nm Level 2 Collection 6.1 aerosol data available at spatial resolution 10 x 10 km (nadir) was acquired from MODIS onboard Terra and Aqua EOS, LAADS DAAC atmosphere archive for the period 2016-2020. MODIS collects AOD data, a columnar retrieved parameter that represents the integral of total light extinction from the surface to the top of the atmosphere. Deep blue algorithm determines the aerosol number in the atmosphere including its properties over bright land surfaces (https://deepblue.gsfc.nasa.gov/science). Quality assurance flag 2, 3 indicate retrieval of AOD for 60-90% and >90% cloud screened pixels respectively. Therefore, for this study, MODIS Terra (overpass 10:30 am LST) and Aqua (overpass 1:30 p.m. LST) Deep Blue AOD at 550nm Land Best Estimate at Quality flag=2, 3 data were extracted and averaged for days, months and year.

To evaluate the uncertainty level of MODIS AOD 550 nm over BV, the daily mean MODIS AOD 550 nm is compared with the daily mean of AERONET AOD 550 nm of Dibrugarh for the year 2018. MODIS-AOD products over land show expected uncertainty of 0.05 ± 0.15 while several global analyses on validation using AERONET (Aerosol Robotic Network) locations confirmed that about 72% of MODIS-AOD retrievals were within the above uncertainty [29].

2.2.2 Reanalysis data

ERA5 ECMWF meteorological data

The hourly estimates of the meteorological variables- AT at 2m, Ps, RH, and u and v component of wind a.g.l., at pressure level 1000 hPa were downloaded and extracted for 3 ground-based stations, namely Dibrugarh, Guwahati and Lakhimpur from ERA5 ECMWF reanalysis data. The hourly estimates were extracted at their native spatial resolution 0.25º x 0.25º, for the period 2016 to 2018.

ERA5 reanalysis combines model data with surface observations from across the world into a globally complete and consistent dataset using advanced modelling and data assimilation systems. The availability, ease of accessibility and high temporal and spatial resolution makes this dataset suitable for the study.

MERRA-2 aerosol components

Hourly estimates of five major aerosol components, namely black carbon (BC), dust (DU2.5), sea salt ($SS_{2.5}$), sulfate (SO_4), and organic carbon (OC) surface concentrations were downloaded and extracted at the horizontal native grid of 0.5º x 0.625º, from the MERRA-2 atmospheric reanalysis for Tezpur station. The hourly estimates of all the major aerosol components were used to calculate the hourly PM2.5 surface concentration (using eq.1) of the Tezpur station for validation purpose. Further, for the generation of PM2.5 spatial variation map over BV, the monthly mean of PM2.5 was calculated using the monthly estimates of the aerosol components (using eq.1, section 2.3.1).

MERRA-2 (M2T1NXAER) is an hourly time-stamped 2-dimensional data assimilation of Aerosol Diagnostics. This assimilation consists of the surface mass concentration of aerosol components BC, $DU_{2.5}$, $SS_{2.5}$, SO_4, and OC. MERRA-2 provides diverse aerosol components at high data quality- continuous spatial and temporal (hourly, monthly)

resolution. Because of these advantages, MERRA-2 aerosol components are extensively used for the calculation of total PM2.5 surface concentration across the globe [30, 31, 32].

2.2.3 Ground-based data

Meteorological Data

3-hourly observations of meteorological parameters- RH, AT, Ps, and WS- were acquired for 3 ground-based stations, namely Guwahati, Dibrugarh and Lakhimpur across the BV (Figure 2.1) for the period 2016 to 2018. These data were acquired from Indian Meteorological Department IMD, Pune.

PM2.5 surface concentration

Ground observation of hourly PM2.5 concentration was obtained from Modelling of Atmospheric Pollution and Networking (MAPAN), Department of Environmental Science Tezpur University, Tezpur (Figure 2.1) for the period 2014 to 2017. The instrument deployed for the ground sampling works on the beta absorption method (BAM), and is calibrated manually as required.

AERONET AOD 500 nm

AOD 500 nm Level 2.0 data were acquired from Aerosol Robotic Network (AERONET) for the Dibrugarh station (Figure 2.1) for the year 2018. AERONET Version 3(V3) AOD 500 nm Level 2.0 data are pre- and post-field calibrated, cloud-screened and quality-assured. Near-real-time estimated uncertainty of V3 Level 2.0 AOD is +0.002 bias with a standard deviation ±0.02 SD [33].

2.2.4 Data pre-processing

Collocation of data

For calculation of PM2.5 surface concentration, hourly estimates of all the 5 major aerosol components available at native spatial resolution 0.5^{o} x 0.625^{o} were made to coincide spatially and temporally with the Tezpur station taking coordinates as the centroid of the grid and matched time window. The daily mean of MERRA-2 PM2.5 estimates was validated with the PM2.5 ground-based observations for the Tezpur station using R^2, RMSE, m (slope) and y-intercept.

Data integration

For the validation purpose, ERA5 meteorological variables were extracted and georeferenced to the corresponding ground-based stations, namely Dibrugarh, Lakhimpur and Guwahati. Ground-based meteorological data were averaged over the time window of 3 to 21 h UTC to represent the daily mean. Similarly, the daily mean of ERA5 meteorological data was calculated for the 3 ground-based stations. The daily mean of WS was calculated from u and v components of wind at 10 m a.g.l. for the corresponding ground stations. The performance of the daily mean of ERA5 meteorological products was assessed with reference to ground-based data for the 3 stations using R^2, RMSE, m (slope) and y-intercept.

The monthly mean of ERA5 meteorological variables and MERRA-2 aerosol components (SO_4, BC, $DU_{2.5}$, $SS_{2.5}$, and OC) were extracted for BV, for the period 2016-2020, for correlation analysis and variability mapping. The monthly mean of AOD 550 nm was calculated by using the daily mean of combined MODIS Terra and Aqua AOD 550 nm data. ERA5 meteorological variables, AOD 550 nm and MERRA-2 aerosol components are available at different spatial resolutions. ERA5 meteorological variables, MODIS AOD 550 nm and MERRA-2 aerosols components were spatially arranged into a new target grid of 0.25º x 0.25º using the Kriging technique. MODIS AOD 550 nm and MERRA-2 aerosol data were re-gridded from their native grid size of 10 x10 km and 0.5º x 0.625º respectively to 0.25º x 0.25º to match the grid size of the available ERA5 ECMWF meteorological product. MERRA-2 aerosols components and MODIS AOD 550 nm data were spatially matched by centroid (latitude and longitude) of ERA5 ECMWF meteorological data for the re-gridding purpose.

Based on the seasonality of meteorological conditions over the study area, MERRA-2 PM2.5 surface concentration and ERA5 meteorological variables were grouped and averaged for four seasons- winter, pre-monsoon, monsoon, and post-monsoon. The seasonal and inter-annual variation maps for PM2.5 surface concentration, AOD 550 nm and meteorological variables were developed at the valley-site scale employing the Kriging technique, spatial and geostatistical analysis tools on ArcGIS 10.5 interface. Kriging (also known as Gaussian process regression) is a widely accepted technique for spatial interpolation of air quality parameters [34].

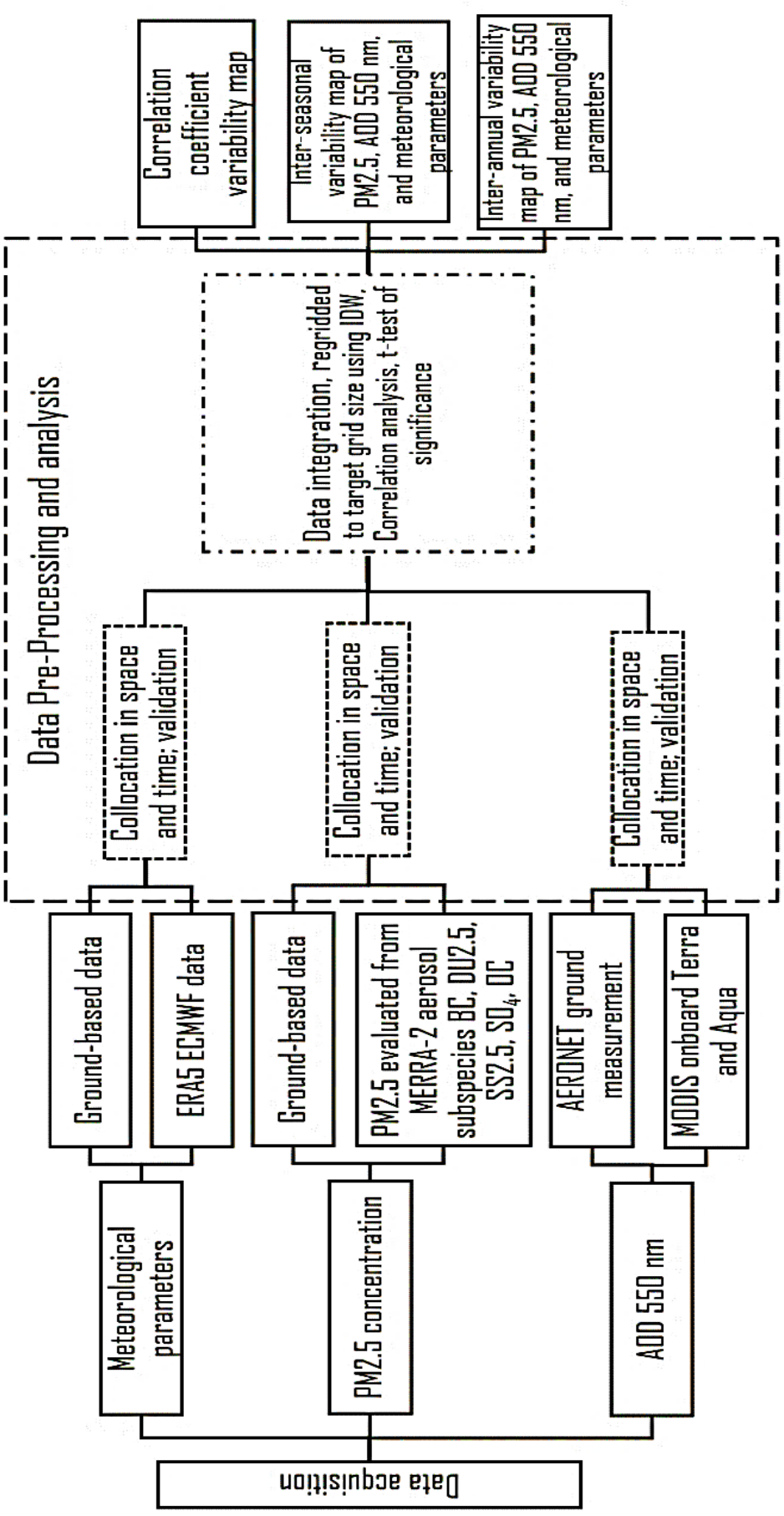

Figure 2.2 Schema of methodology.

2.3 METHODOLOGY

The schema of the methodological framework is illustrated in Figure 2.2 and the details are discussed in the following sub-sections.

2.3.1 Calculation of total PM2.5 surface concentration

MERRA-2 major aerosol components SO_4, BC, $DU_{2.5}$, $SS_{2.5}$, and OC surface concentrations were used to calculate total PM2.5 surface concentrations using Hand et al. (2011) [35] equation as given below-

$$PM2.5=1.375 \times [SO_4] + 1.8 \times [OC] + [BC] + [DU_{2.5}] + [SS_{2.5}] \quad (1)$$

Total PM2.5 surface mass concentration is usually calculated as the sum of inorganic ions, organic matter, black carbon, dust and sea salt. The principal components of inorganic ions are SO_4, NO_3 and NH_4. In cases NO_3 and NH_4 data are absent or inaccurate SO_4 is multiplied by 1.375 to represent inorganic ions, as $(NH_4)_2SO_4$ contains 73 percent SO_4 by mass [36, 37]. Similarly, OC is used as a surrogate for organic matter by multiplying with coefficients 1.6 ± 0.2 for urban particles and 2.1 ± 0.2 for aged (non-urban) particles. For biomass burning particles, the coefficient can be as high as 2.6 [37-38]. These coefficient values are derived from numerous experiments. The coefficient for OC in the equation (1) is used according to the particle characteristics over BV.

2.3.2 Validation of data

It is essential to validate the satellite and reanalysis derived data with respect to ground-based observations before using it for analysis. The validation is done to estimate the data products' performance, accuracy and uncertainty over a particular geographic area. The performance of MODIS AOD 550 nm, ERA5 meteorological variables and MERRA-2 PM2.5 estimates were assessed with reference to AERONET AOD 500 nm, IMD meteorological data and MAPAN PM2.5 respectively. For validation purpose, days with at least 18 hours of data available (i.e., 75 percent of 24 hours) were chosen for the calculation of the daily mean of the parameters. The period for data validation was chosen according to data availability.

The monthly mean of MODIS AOD 550 nm retrievals was validated with reference to the daily mean AERONET AOD 500 nm of Dibrugarh station for 2018. The daily mean of ERA5 meteorological variables AT, RH, Ps and WS were verified with reference to the

daily mean of ground-based meteorological data of Guwahati, Lakhimpur and Dibrugarh for 2016-2018. Similarly, the daily mean of MERRA-2 PM2.5 was validated with reference to ground-based PM2.5 data for Tezpur station, 2014-2017. For validation purpose, statistical parameters viz. m (slope), y-intercept, coefficient of determination (R^2) and root mean square error (RMSE) were used. R^2 indicates the proportion of the variation in the response variable that is caused by the independent variable. It is an expression of the goodness of fit.

2.3.3 Correlation analysis and significance test

The strength of linearity between two variables is measured using Pearson correlation analysis. The coefficient ranges from -1 to 1 indicating a total negative linear correlation to a total positive linear correlation. Pearson correlation analysis was performed to investigate how PM2.5 is associated with individual meteorological parameters- AT, RH, Ps and WS. A t-test was performed to measure the statistical significance of the correlation coefficients.

2.4 RESULTS AND DISCUSSION

2.4.1 Performance assessment of MERRA-2 PM2.5 with reference to ground-based data

The performance of the daily mean of MERRA-2 PM2.5 surface concentration was assessed with the corresponding ground observations of the Tezpur station (Figure 2.3a). The weak R^2 value of 0.283 and RMSE value of 30.53 $\mu g/m^3$ (Figure 2.3a) indicated the limitation of MERRA-2 PM2.5 estimates over BV. The terrain complexity of BV along with cloudy weather may restrict the assimilation of MERRA-2 aerosol products. Further, the lack of nitrate in the MERRA-2 PM2.5 aerosol assimilation may explain the estimation efficacy.

Additionally, the monthly mean of both ground-based and MERRA-2 PM2.5 surface concentrations was plotted, for the period 2014 to 2017, to represent the magnitude of monthly variation. MERRA-2 PM2.5 mean values have shown similar variation with ground-based PM2.5 (Figure 2.3b).

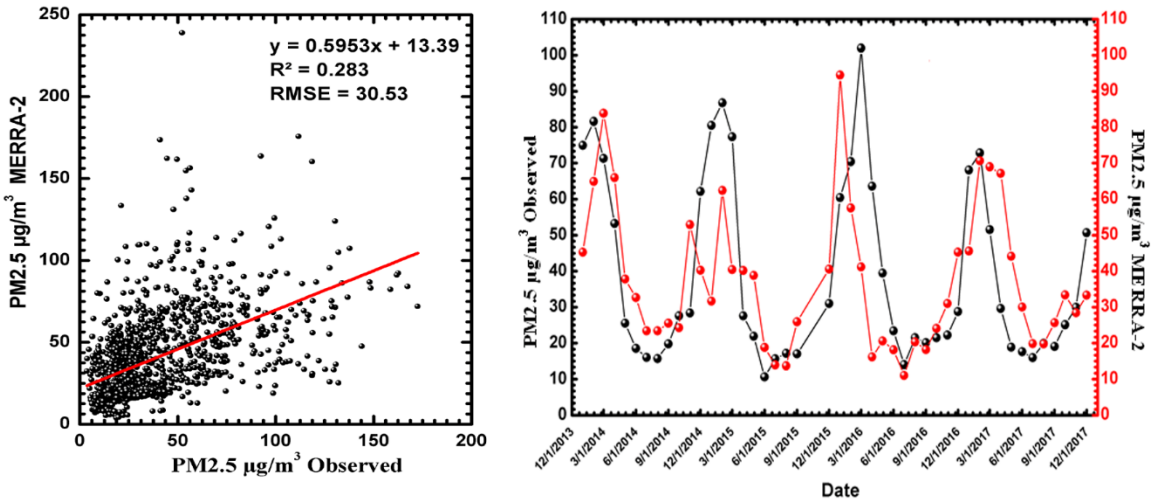

Figure 2.3 (a) Performance assessment of MERRA-2 PM2.5 with reference to ground-based data of Tezpur (b) Monthly mean variation of MERRA-2 PM2.5 and ground-based PM2.5 concentration, 2014-2017.

2.4.2 Performance assessment of ERA5 ECMWF reanalysis meteorological data with reference to ground-based data

The daily mean of ERA5 meteorological variables was compared with that of the ground-based meteorological measurements of Dibrugarh, Lakhimpur and Guwahati stations (Figure 2.4). R^2 and RMSE values for AT (R^2 = 0.88 to 0.91; RMSE= 0.00048 to 0.12), Ps (0.52 to 0.95; 0.101 to 0.230), RH (0.59 to 0.67; 0.230 to 0.366) and WS (0.20 to 0.30; 0.004 to 0.032) were estimated for the ground stations. High R^2 values and low RMSE for AT, RH, and Ps suggest the viability of ERA5 ECMWF meteorological variables over the complex terrain of BV. The moderate R^2 value for WS, on the other hand, suggests that WS calculated from u and v components of wind could moderately represent the prevalent WS over the valley. The performance of ERA5 WS may be attributed to the local topography of the valley where wind speed varies at small space and time scales impacted by the hill ranges and vegetation density.

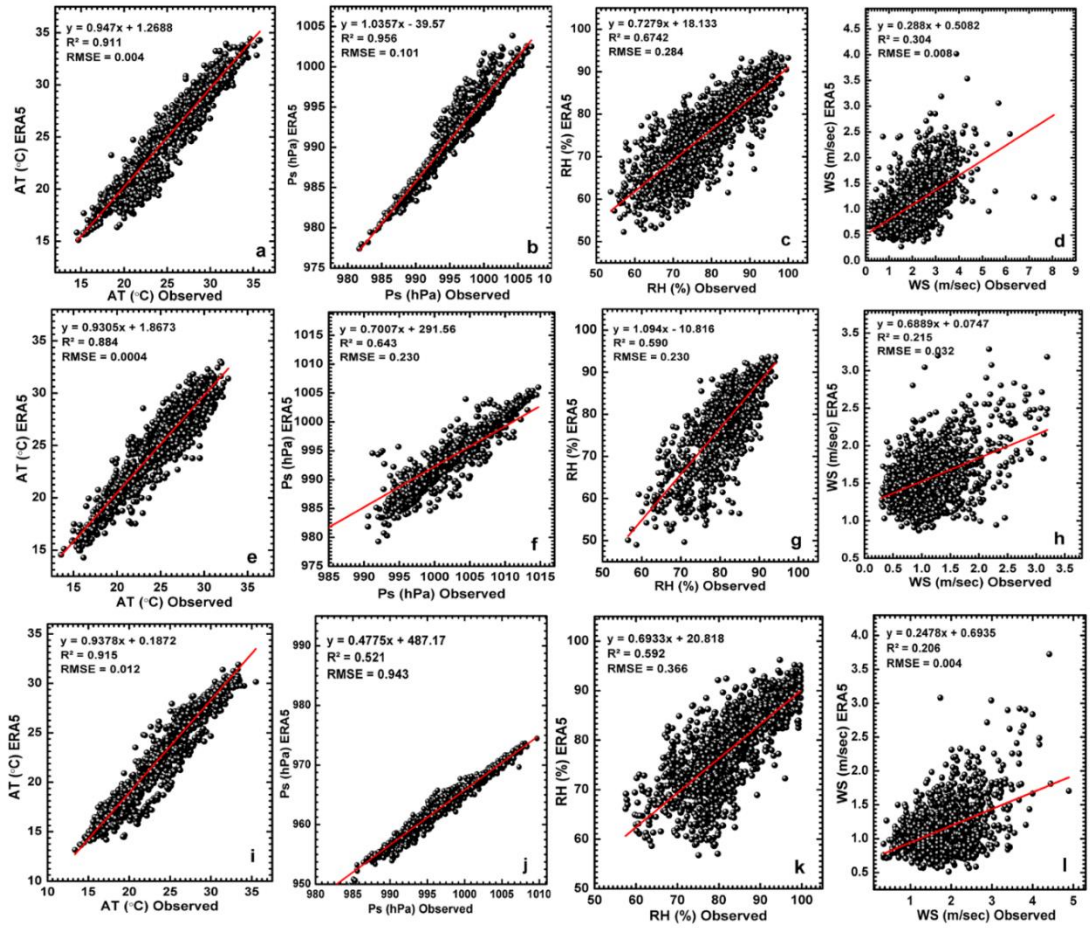

Figure 2.4 Scatter plots showing performance of daily mean ERA5 reanalysis meteorological products- air temperature (AT), surface pressure (Ps), relative humidity (RH) and wind speed (WS) with reference to ground-based meteorological data for 3 different stations- (a-d) Guwahati, (e-h) Dibrugarh (i-l) Lakhimpur over Brahmaputra valley, 2016-2019.

2.4.3 Performance assessment of MODIS AOD 550 nm with reference to ground-based data

The daily mean of MODIS AOD 550 nm was compared to AERONET AOD 500 nm of the Dibrugarh station. MODIS AOD 550 nm well represented the ground measurements of AERONET AOD 550 nm with R^2 value of 0.977, y-intercept 0.954 and RMSE 0.00028 (Figure 2.5).

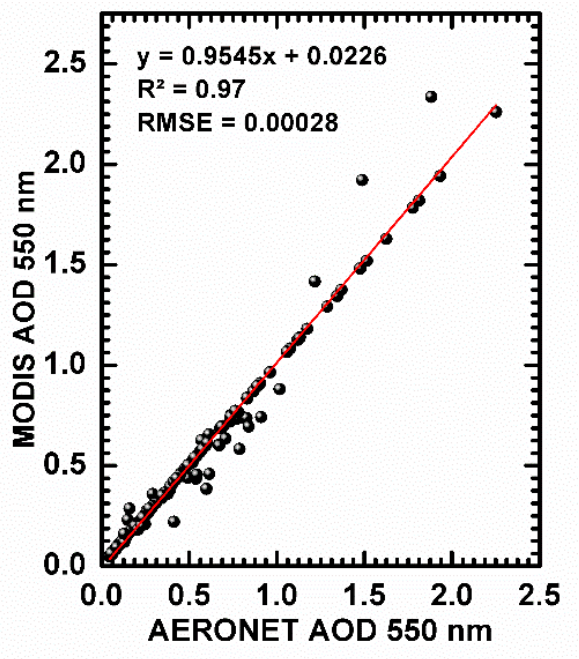

Figure 2.5 Performance assessment of MODIS AOD 550 nm with reference to ground-based AERONET AOD 500 nm data for Dibrugarh station, 2018 -2019.

2.4.4 Spatial and seasonal variation of PM2.5, AOD 550 nm and the meteorological parameters

RH varied greatly in magnitude on a spatial and seasonal scale over BV (Figure 2.6a1-a4). An east-west decreasing trend in RH was observed from east to west for all seasons except in monsoon, during which the eastern and central parts of the valley showed higher relative humidity than that of the western. RH varied by the pattern of vegetation density distribution [39]. Seasonally, as expected, monsoon had the highest relative humidity (88.52% - 81.01 %) followed by post-monsoon (81.65% - 62.31%), pre-monsoon (82.93% - 74.85%), and winter (76.10% - 64.15%).

AT drops from west to east during the pre-monsoon season. However, for other seasons there was no clear pattern. The appreciable lower temperature was observed along the foothills and densely vegetated areas over the valley. AT was noted highest during the monsoon (29.27ºC - 23.31ºC), followed by pre-monsoon (26.20ºC - 18.84 ºC), post-monsoon (23.08ºC - 16.53 ºC), and winter (18.90ºC - 11.38 ºC) (Figure 2.6b1-b4).

Ps varied considerably seasonally and spatially. High Ps was observed over the eastern part than the western. Winter (1002.51 hPa - 879.78 hPa) had the highest Ps, followed by post-monsoon (1001.58 hPa - 880.39 hPa), pre-monsoon (995.55 hPa - 875.93 hPa) and

monsoon (990.83 hPa - 873.20 hPa) (Figure 2.6c1-c4). Seasonal variations in the atmospheric pressure system are most likely driven by the orographic configurations and atmospheric processes in the valley. Ps temporal variability was more noticeable than its spatial variance. However, the spatial and temporal variation pattern of Ps synergizes with AT for all seasons.

PM2.5 surface concentration over the western and central parts of BV was higher than that of the eastern part (Figure 2.6d1-d4). Because the western and central parts of BV are closer to BoB and IGP, the residue of the winter haze blown from IGP results in increased aerosols over these parts [8, 9]. The population density distribution, prevailing meteorological conditions and topographical orientation appear responsible for the east-west trending asymmetry of PM2.5. Seasonally, PM2.5 concentration was observed to be the highest (78.79 $\mu g/m^3$ - 38.65 $\mu g/m^3$) during the winter, followed by pre-monsoon (69.14 $\mu g/m^3$ - 47.27 $\mu g/m^3$), post-monsoon (50.03 $\mu g/m^3$ - 9.47 $\mu g/m^3$), and monsoon (25.66 $\mu g/m^3$ - 11.90 $\mu g/m^3$). Heavy monsoonal rainfall during monsoon is effective in washing out the dust particles reducing PM2.5 surface concentration.

AOD 550 nm was relatively high over the western part of BV than that of the central and eastern parts. Areas with high AOD loading coincide with high PM2.5 surface concentration for all the seasons except pre-monsoon. AOD 500 nm was observed highest in winter (1.02-0.21) followed by pre-monsoon (0.68-0.26), monsoon (0.66-0.19) and post-monsoon (0.48- 0.088) (Figure 2.6e1-e4). AOD 550 nm was found the least in post-monsoon.

WS generally was stronger in the western and central regions of the BV than in the eastern parts (Figure 2.6f1-f4). However, in the winter season, WS was lower in the central part as compared to the other parts (Figure 2.6f1). Westerlies, brought by the south-west monsoon through the western opening, predominates over BV during the pre-monsoon and monsoon. It is quite apparent that the local orographic factors of the surrounding hilly landscape cause the asymmetrical distribution of wind speed across the valley during all the seasons. Low WS prevailed over BV in all the seasons- monsoon WS (0.20 to 2.28 m/sec), followed by pre-monsoon (1.751 to 0.197 m/sec), post-monsoon (0.18 to 1.65 m/sec), and winter (1.34 to 0.28 m/sec) (Figure 2.6f1-f4).

Pronounced seasonal and spatial variability of meteorological parameters, AOD 550 nm and PM2.5 surface concentration over the valley during the study period was evident

(Figure 2.6 and Table 2.4). The spatial pattern of PM2.5 and AOD 550 nm variation is in conformity with the topographic orientation, vegetation density distribution, population density and local wind circulation pattern.

Table 2.4 Descriptive statistics of the meteorological parameters, PM2.5 µg/m^3 and AOD 550 nm of the entire Brahmaputra valley for different seasons, 2016-2020.

Seasons	Statistics	RH (%)	AT (ºC)	WS (m/sec)	Ps (hPa)	AOD 550 nm	PM2.5 (µg/m^3)
Winter	Min	59.05	25.26	0.23	923.31	0.33	46.80
	Max	77.24	29.51	1.13	1016.78	1.02	71.44
	Mean	67.97	28.45	0.51	996.08	0.62	58.36
	Median	67.65	28.75	0.48	1001.55	0.61	58.19
	SD	4.67	0.89	0.17	16.90	0.17	5.85
Pre-monsoon	Min	67.27	18.62	0.20	919.11	0.05	32.53
	Max	77.92	26.11	1.46	1010.14	0.69	82.76
	Mean	72.11	24.33	0.70	990.14	0.53	58.21
	Median	71.99	24.51	0.64	995.37	0.55	57.39
	SD	2.63	1.55	0.26	16.43	0.13	11.71
Monsoon	Min	79.41	25.26	0.21	914.80	0.02	10.11
	Max	87.36	29.51	1.84	1003.98	0.52	25.80
	Mean	84.07	28.45	0.79	984.29	0.18	17.57
	Median	84.02	28.75	0.74	989.53	0.11	17.42
	SD	1.45	0.89	0.43	16.17	0.16	4.08
Post-monsoon	Min	62.83	18.80	0.18	922.44	0.02	10.02
	Max	81.28	23.23	1.60	1014.44	0.47	52.29
	Mean	72.39	22.11	0.54	994.08	0.28	27.48
	Median	72.36	22.39	0.47	999.44	0.29	26.95
	SD	4.42	0.93	0.30	16.61	0.10	10.59

WS= Wind speed, RH= Relative humidity, Ps= Surface Pressure, AT= Air temperature, AOD 550 nm= Aerosol Optical Depth at 550 nm, PM2.5= particulate matter <2.5µm aerodynamic diameter.

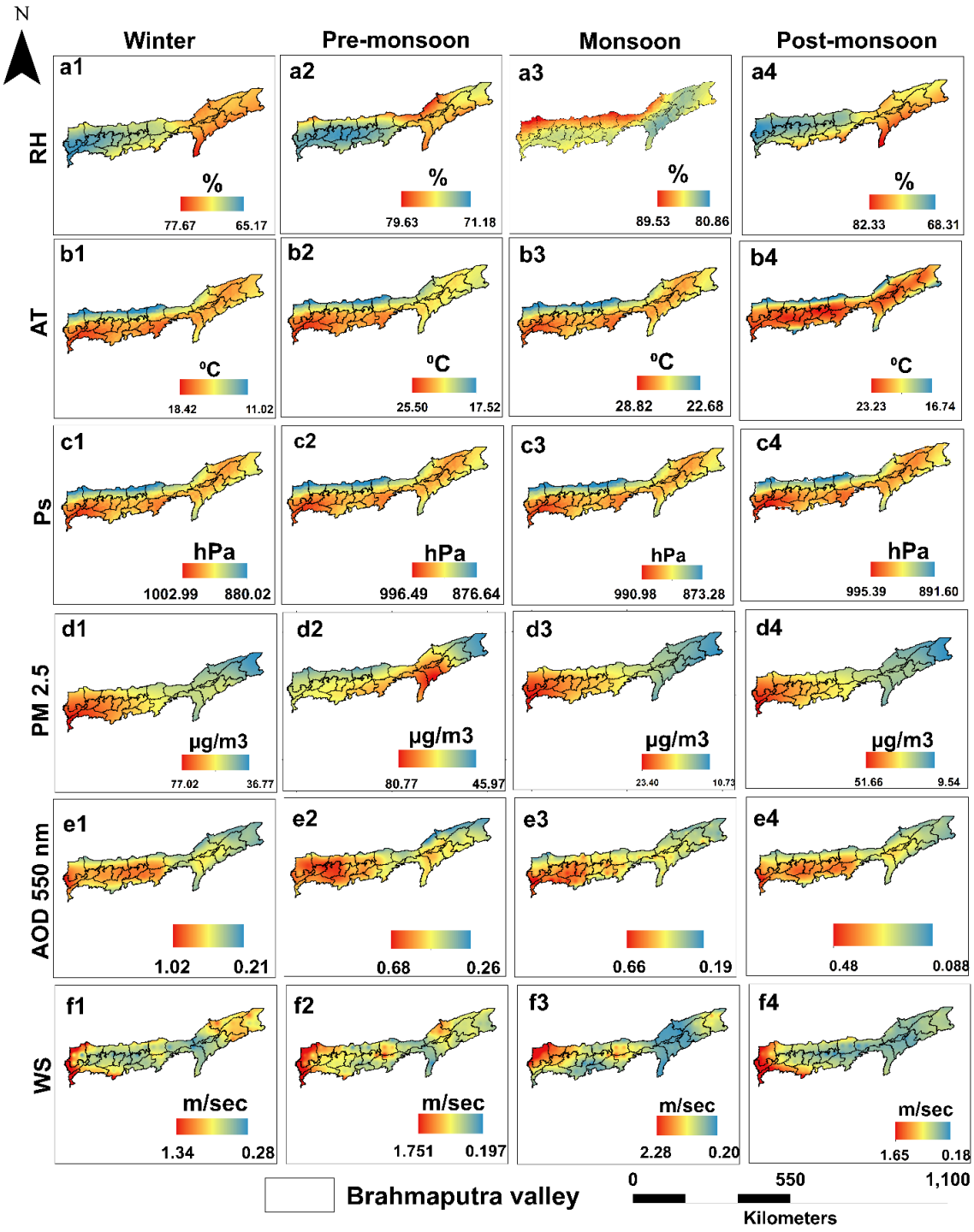

Figure 2.6 Spatial variation of seasonal mean of (a1-a4) relative humidity (RH), (b1-b4) air temperature (AT), (c1-c4) surface pressure (Ps), (d1-d4) PM2.5 µg/m^3, (e1-e4) AOD 550 nm (f1-f4) and wind speed (WS) over Brahmaputra valley, 2016-20

2.4.5 Inter-annual variation of PM2.5, AOD 550 nm and meteorological parameters

The inter-annual variability of meteorological parameters was minimal during the study period, 2016-2020 (Figure 2.7). In 2017, RH showed a small difference in the minima-maxima range as compared to that of the other years (Figure 2.7a1-a5). In 2018, PM2.5 surface concentration was found to be the highest (Figure 2.7d3). Except for 2017, the AOD 550 nm value increased from 2016 to 2020. In 2020, the valley had the highest AOD 550 nm (0.74-0.15) (Figure 2.7e5). In 2020, the highest magnitudes of all meteorological parameters were observed over the valley.

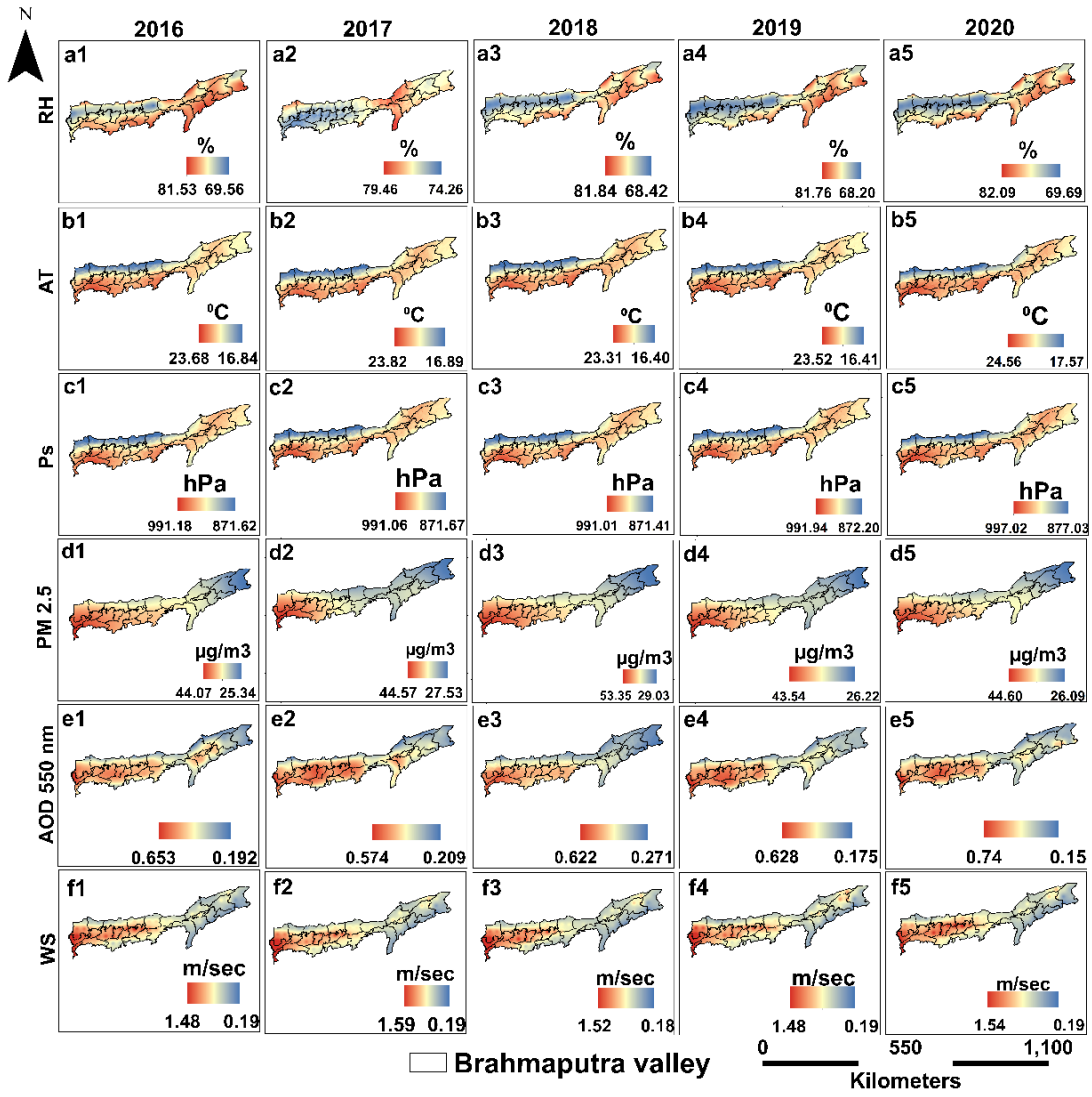

Figure 2.7 Inter-annual variation of (a1-a5) relative humidity (RH), (b1-b5) air temperature (AT), (c1-c5) surface pressure (Ps), (d1-d5) PM2.5 µg/m^3, (e1-e5) AOD 550 nm and (f1-f5) wind speed (WS) over Brahmaputra valley, 2016-2020.

2.4.6 PM2.5-AOD-Meteorology relationship analysis

Moderate to strong negative correlation between PM2.5 and AT (r= -0.41 to -0.75, $p<0.05$) was observed (Figure 2.8a) over the BV. The magnitude was comparatively stronger in the western part (r= -0.56 to -0.68, $p<0.05$). The negative correlation between the two parameters indicates the occurrence of two possible processes. Firstly, diffusion of PM2.5 surface concentration by strong thermal turbulence driven by high temperature [40]. Secondly, the organic precursors emitted from biomass burning and fossil fuel combustion shift from the particle phase to the gas phase due to their volatility with increasing temperature, [41, 42] thus reducing the PM2.5 surface concentration.

PM2.5-RH were negatively correlated. The correlation showed variation throughout the valley. The central parts of BV were noted with stronger negative correlation (r= -0.79, $p>0.05$) as compared to the eastern (r= -0.50 to -0.57, $p<0.05$) and western parts (r= -0.60 to 0.70, $p<0.05$) (Figure 2.8b). The variation in magnitude could be due to the presence of non-hygroscopic organic carbon (OC) in PM2.5 surface concentration.

PM2.5-Ps relationship was positive and the coefficient ranged from r= 0.18 to r= 0.68 ($p<0.05$) over BV. The positive relation indicates that PM2.5 concentration increases with surface pressure (Figure 2.8c). Liu et al. (2020) [43] had reported similar findings for China, where NO_2, and O_3 precursors of total PM2.5 was positively correlated with surface pressure.

PM2.5-AOD 550 nm correlation coefficients (r) varied widely from 0.13 to 0.74 ($p<0.05$) (Figure 2.8d). A strong positive correlation (r= 0.54 to 0.74; $p<0.05$) was observed in some areas of the central and eastern valley, whereas a moderate to weak positive correlation (r= 0.13 to 0.53, $p<0.05$) was observed in the western parts. PM2.5 and AOD 550 nm relation over the BV varied according to the proximity of emission sources and the ecology of the area. A weak to moderate correlation was observed in the western part where the dust aerosols blown from the IGP region prevails; whilst a strong correlation was observed over areas with high vegetation density, national parks and agricultural fields (typical agroecosystem) [39] where biogenic aerosols may predominate. The large variation in the PM2.5-AOD 550 nm relationship may be due to changes in the extinction efficiency of hygroscopic aerosols from high to low humid areas [44, 45, 46, 47].

PM2.5-WS relationship was found to be weak negative to strong positive (r= -0.18 to 0.71; p<0.05) over BV (Figure 2.8e). While moderate to a strong positive association (r= 0.32 to 0.71, p<0.05) was observed over the western and some areas of the central parts of BV, weak positive to a negative association (r= -0.18 to 0.39, p<0.05) existed in the eastern part of the valley.

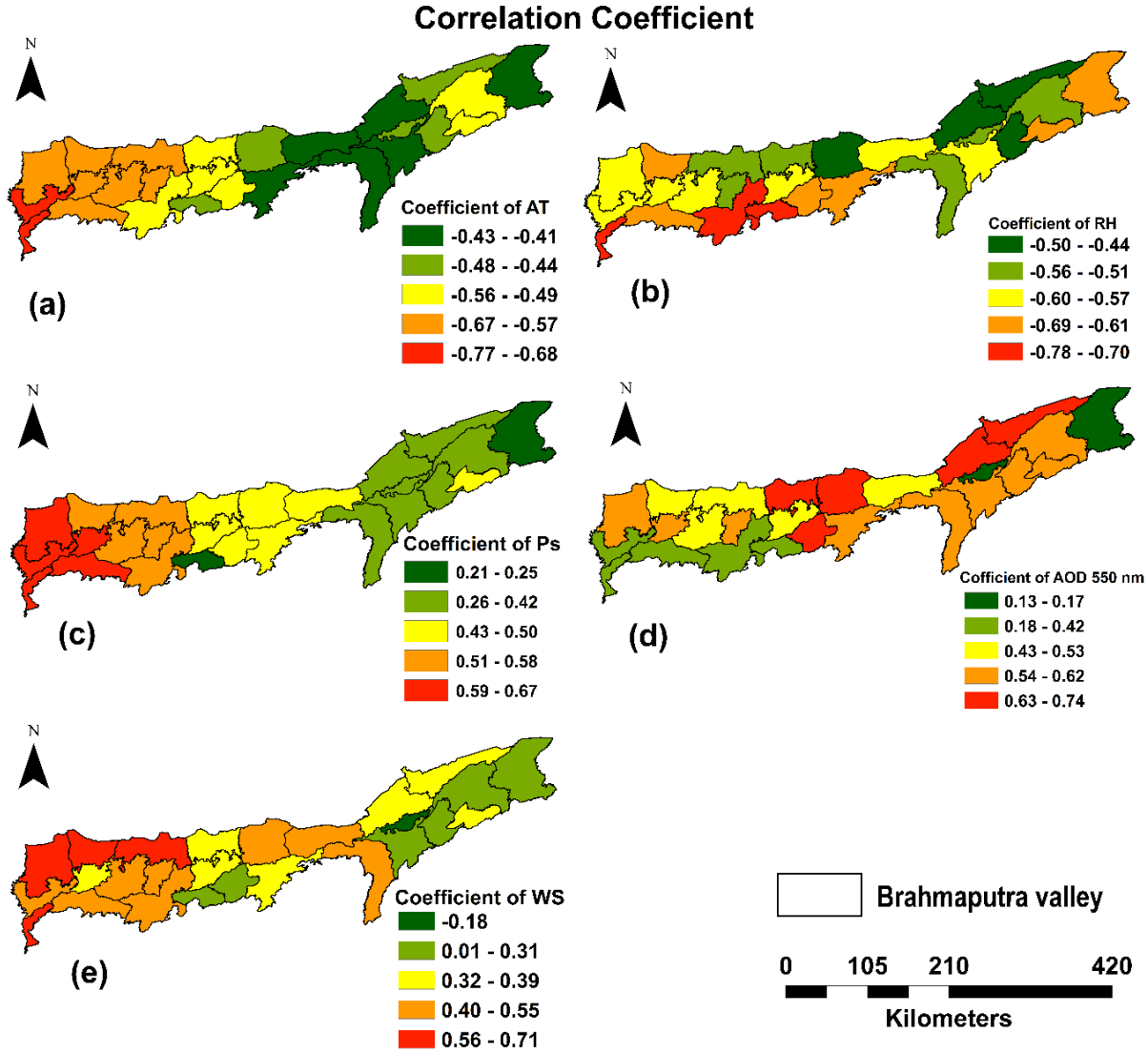

Figure 2.8 Correlation coefficient of (a) air temperature (AT), (b) relative humidity (RH), (c) surface pressure (Ps), (d) AOD 550 nm and (e) wind speed (WS), with PM2.5 concentration over Brahmaputra valley, 2016-2020. Except for one grid point at central BV, all the correlations are statistically significant at 0.05 level (two-tailed) (p<0.05).

2.5 CONCLUSION

This study gleans major insights into the spatial, seasonal and inter-annual variation pattern of PM2.5, AOD 550 nm and meteorological parameters viz. AT, WS, Ps and RH, and the nature and strength of PM2.5-AOD-meteorology relationship over BV at the valley-site scale. PM2.5 surface mass concentration, AOD 550 nm as well as meteorological factors showed prominent spatio-temporal variation across the valley. Pronounced east-west trending asymmetry was observed in the spatial distribution of all the parameters. For PM2.5 eastern part of BV showed notably lower surface concentration compared to that of the central and western parts. During the monsoon season, the specific topography combined with the local meteorological conditions and heavy washout results in a cleaner environment. High PM2.5 concentration areas were found to coincide with high AOD 550 nm except for pre-monsoon. The inter-annual variation in AT, RH, Ps, WS, AOD 550 nm and PM2.5 is small over BV.

PM2.5 showed moderate to strong negative correlation with AT and RH whilst positive relation with Ps and AOD 550 nm over BV. A weak negative to strong positive PM2.5-WS relationship was observed over the valley. Results reveal that non-hygroscopic organic precursor and carbonaceous aerosols may be present in good proportion in total PM2.5 surface concentration. Columnar AOD 550 nm and surface PM2.5 showed varying correlation coefficients, poor to strong, from highly humid to less humid areas.

This work also evaluates the efficacy of MERRA-2 aerosol products and ERA5 reanalysis meteorological variables over an intermontane valley. MERRA-2 PM2.5 estimate moderately represents the ground observations for the Tezpur station with an uncertainty of 30.53 $\mu g/m^3$. Complex terrain, presence of cloud cover and lack of nitrate aerosols in the GOCART model could partly explain the estimation efficacy of MERRA-2 PM2.5. Except for wind speed, the other ERA5 meteorological variables-AT, RH, and Ps well-represented the ground-based observations for all the three stations- Dibrugarh, Guwahati and Lakhimpur across the BV. WS computed from ERA5 u and v component of wind at 10 m a.g.l, moderately represented the predominant local WS. ERA5 ECMWF reanalysis meteorological data was proven to be viable for the valley.

Besides the analysis of the relationship and the spatio-temporal variability of the parameters, this study is an important step towards overcoming the data limitations for

aerosol studies over the complex terrain of BV through the survey of the data sources, their performance assessment and integration.

2.6 REFERENCE

[1] Han, S., Bian, H., Zhang, Y., Wu, J., Wang, Y., Tie, X., Li, Y., Li, X., and Yao, Q. Effect of aerosols on visibility and radiation in spring 2009 in Tianjin, China. *Aerosol and Air Quality Research*, 12(2):211-217, 2012.

[2] Pope I, C. A., Burnett, R. T., Thun, M. J., Calle, E. E., Krewski, D., Ito, K., and Thurston, G. D. Lung cancer, cardiopulmonary mortality, and long-term exposure to fine particulate air pollution. *Jama*, 287(9):1132-1141, 2002.

[3] World Health Organization. Health aspects of air pollution with particulate matter, ozone and nitrogen dioxide: report on a WHO working group, Bonn, Germany 13-15 January 2003. Copenhagen: WHO Regional Office for Europe.

[4] Harrison, R. M., Giorio, C., Beddows, D. C., and Dall'Osto, M. Size distribution of airborne particles controls outcome of epidemiological studies. *Science of The Total Environment*, 409(2):289-293, 2010.

[5] Brown, J. S., Gordon, T., Price, O., and Asgharian, B. Thoracic and respirable particle definitions for human health risk assessment. *Particle and Fibre Toxicology*, 10(1):1-12, 2013.

[6] Hoff, R. M. and Christopher, S. A. Remote sensing of particulate pollution from space: have we reached the promised land? *Journal of the Air & Waste Management Association*, 59(6):645-675, 2009.

[7] Gogoi, M. M., Pathak, B., Moorthy, K. K., Bhuyan, P. K., Babu, S. S., Bhuyan, K., and Kalita, G. Multi-year investigations of near surface and columnar aerosols over Dibrugarh, northeastern location of India: Heterogeneity in source impacts. *Atmospheric Environment*, 45(9):1714-1724, 2011.

[8] Pathak, B., Borgohain, A., Bhuyan, P. K., Kundu, S. S., Sudhakar, S., Gogoi, M. M., and Takemura, T. Spatial heterogeneity in near surface aerosol characteristics across the Brahmaputra valley. *Journal of Earth System Science*, 123(4):651-663, 2014.

[9] Tiwari, S., Dumka, U. C., Gautam, A. S., Kaskaoutis, D. G., Srivastava, A. K., Bisht, D. S., Chakrabarty, R. K., Sumlin, B. J., and Solmon, F. Assessment of $PM_{2.5}$ and PM_{10} over Guwahati in Brahmaputra River Valley: Temporal evolution, source apportionment and meteorological dependence. *Atmospheric Pollution Research*, 8(1):13-28, 2017.

[10] Bhuyan, P., Deka, P., Prakash, A., Balachandran, S., and Hoque, R. R. Chemical characterization and source apportionment of aerosol over mid Brahmaputra valley, India. *Environmental Pollution*, 234:997-1010, 2018.

[11] Bonasoni, P., Laj, P., Marinoni, A., Sprenger, M., Angelini, F., Arduini, J., Bonafè, U., Calzolari, F., Colombo, T., Decesari, S., and Di Biagio, C. Atmospheric Brown Clouds in the Himalayas: first two years of continuous observations at the Nepal Climate Observatory-Pyramid (5079 m). *Atmospheric Chemistry and Physics*, 10(15):7515-7531, 2010.

[12] Sarkar, C., Chatterjee, A., Singh, A. K., Ghosh, S. K., and Raha, S. Characterization of black carbon aerosols over Darjeeling- A high altitude Himalayan station in eastern India. *Aerosol and Air Quality Research*, 15(2):465-478, 2015.

[13] Arya, S. P. *Air pollution meteorology and dispersion.* New York: Oxford University Press, 1999.

[14] Koch, D., Park, J., and Del Genio, A. Clouds and sulfate are anticorrelated: A new diagnostic for global sulfur models. *Journal of Geophysical Research: Atmospheres*, 108(D24), 2003.

[15] Wise, E. K. and Comrie, A. C. Meteorologically adjusted urban air quality trends in the Southwestern United States. *Atmospheric Environment*, *39*(16):2969-2980, 2005.

[16] Wang, J. and Martin, S. T. Satellite characterization of urban aerosols: Importance of including hygroscopicity and mixing state in the retrieval algorithms. *Journal of Geophysical Research: Atmospheres*, 112(D17), 2007.

[17] Gupta, P. and Christopher, S. A. Particulate matter air quality assessment using integrated surface, satellite, and meteorological products: Multiple regression approach. *Journal of Geophysical Research: Atmospheres*, 114(D14), 2009.

[18] Pateraki, St., Asimakopoulos, D. N., Flocas, H. A., Maggos, T., and Vasilakos, C. The role of meteorology on different sized aerosol fractions (PM_{10}, $PM_{2.5}$, $PM_{2.5-10}$). *Science of the Total Environment*, 419:124-135, 2012.

[19] Jacob, D. J. and Winner, D. A. Effect of climate change on air quality. *Atmospheric Environment*, 43(1):51-63, 2009.

[20] Porter, W. C., Heald, C. L., Cooley, D., and Russell, B. Investigating the observed sensitivities of air-quality extremes to meteorological drivers via quantile regression. *Atmospheric Chemistry and Physics*, 15(18):10349-10366, 2015.

[21] Westervelt, D. M., Horowitz, L. W., Naik, V., Tai, A. P. K., Fiore, A. M., and Mauzerall, D. L. Quantifying PM2.5-meteorology sensitivities in a global climate model. *Atmospheric Environment*, 142:43-56, 2016.

[22] Carmona, J. M., Gupta, P., Lozano-García, D. F., Vanoye, A. Y., Yépez, F. D., and Mendoza, A. Spatial and temporal distribution of $PM_{2.5}$ pollution over northeastern

Mexico: Application of MERRA-2 reanalysis datasets. *Remote Sensing*, 12(14):2286, 2020.

[23] Bali, K., Dey, S., and Ganguly, D. Diurnal patterns in ambient $PM_{2.5}$ exposure over India using MERRA-2 reanalysis data. *Atmospheric Environment*, 248:118180, 2021.

[24] Chakrabarty, R. K., Garro, M. A., Wilcox, E. M., and Moosmüller, H. Strong radiative heating due to wintertime black carbon aerosols in the Brahmaputra River Valley. *Geophysical Research Letters*, 39(9), 2012.

[25] Kumar, A. Variability of aerosol optical depth and cloud parameters over North Eastern regions of India retrieved from MODIS satellite data. *Journal of Atmospheric and Solar-Terrestrial Physics*, 100:34-49, 2013.

[26] Pathak, B., Subba, T., Dahutia, P., Bhuyan, P. K., Moorthy, K. K., Gogoi, M. M., Babu, S. S., Chutia, L., Ajay, P., Biswas, J., and Bharali, C. Aerosol characteristics in north-east India using ARFINET spectral optical depth measurements. *Atmospheric Environment*, 125:461-473, 2016.

[27] Biswas, J., Pathak, B., Patadia, F., Bhuyan, P. K., Gogoi, M. M., and Babu, S. S. Satellite-retrieved direct radiative forcing of aerosols over North-East India and adjoining areas: climatology and impact assessment. *International Journal of Climatology*, 37:298-317, 2017.

[28] Barman, N. and Gokhale, S. Urban black carbon-source apportionment, emissions and long-range transport over the Brahmaputra River Valley. *Science of the Total Environment*, 693:133577, 2019.

[29] Levy, R. C., Remer, L. A., Kleidman, R. G., Mattoo, S., Ichoku, C., Kahn, R., and Eck, T. F. Global evaluation of the Collection 5 MODIS dark-target aerosol products over land. *Atmospheric Chemistry and Physics*, 10(21):10399-10420, 2010.

[30] Buchard, V., Da Silva, A. M., Randles, C. A., Colarco, P., Ferrare, R., Hair, J., Hostetler, C., Tackett, J., and Winker, D. Evaluation of the surface $PM_{2.5}$ in Version 1 of the NASA MERRA Aerosol Reanalysis over the United States. *Atmospheric Environment*, 125:100-111, 2016.

[31] Provençal, S., Buchard, V., da Silva, A. M., Leduc, R., and Barrette, N. Evaluation of PM surface concentrations simulated by Version 1 of NASA's MERRA Aerosol Reanalysis over Europe. *Atmospheric Pollution Research*, 8(2):374-382, 2017.

[32] Navinya, C. D., Vinoj, V., and Pandey, S. K. Evaluation of $PM_{2.5}$ surface concentrations simulated by NASA's MERRA Version 2 aerosol reanalysis over India

and its relation to the air quality index. *Aerosol and Air Quality Research*, 20(6):1329-1339, 2020.

[33] Giles, D. M., Sinyuk, A., Sorokin, M. G., Schafer, J. S., Smirnov, A., Slutsker, I., Eck, T. F., Holben, B. N., Lewis, J. R., Campbell, J. R., and Welton, E. J. Advancements in the Aerosol Robotic Network (AERONET) Version 3 database–automated near-real-time quality control algorithm with improved cloud screening for Sun photometer aerosol optical depth (AOD) measurements. *Atmospheric Measurement Techniques*, 12(1):169-209, 2019.

[34] Jerrett, M., Burnett, R. T., Ma, R., Pope III, C. A., Krewski, D., Newbold, K. B., Thurston, G., Shi, Y., Finkelstein, N., Calle, E. E., and Thun, M. J. Spatial analysis of air pollution and mortality in Los Angeles. *Epidemiology*, 727-736, 2005.

[35] Hand, J. L., Copeland, S. A., McDade, C. E., Day, D. E., Moore, J. C. T., Dillner, A. M., Pitchford, M. L., Indresand, H., Schichtel, B. A., Malm, W. C., and Watson, J. G. Spatial and seasonal patterns and temporal variability of haze and its constituents in the United States, IMPROVE Report V. *Cooperative Institute for Research in the Atmosphere, Fort Collins*, 2011.

[36] Malm, W. C., Sisler, J. F., Huffman, D., Eldred, R. A., and Cahill, T. A. Spatial and seasonal trends in particle concentration and optical extinction in the United States. *Journal of Geophysical Research: Atmospheres*, 99(D1):1347-1370, 1994.

[37] Chow, J. C., Lowenthal, D. H., Chen, L. W. A., Wang, X., and Watson, J. G. Mass reconstruction methods for $PM_{2.5}$: a review. *Air Quality, Atmosphere & Health*, 8(3):243-263, 2015.

[38] Turpin, B. J. and Lim, H. J. Species contributions to $PM_{2.5}$ mass concentrations: Revisiting common assumptions for estimating organic mass. *Aerosol Science & Technology*, 35(1):602-610, 2001.

[39] Forest Survey of India. India State of Forest Report 2019. Retrieved from https://fsi.nic.in/isfr19/vol2/isfr-2019-vol-ii-assam.pdf

[40] Tian, G., Qiao, Z., and Xu, X. Characteristics of particulate matter (PM_{10}) and its relationship with meteorological factors during 2001–2012 in Beijing. *Environmental Pollution*, 192:266-274, 2014.

[41] Dawson, J. P., Adams, P. J., and Pandis, S. N. Sensitivity of $PM_{2.5}$ to climate in the Eastern US: a modeling case study. *Atmospheric Chemistry and Physics*, 7(16):4295-4309, 2007.

[42] Tsigaridis, K. and Kanakidou, M. Secondary organic aerosol importance in the future atmosphere. *Atmospheric Environment*, 41(22):4682-4692, 2007.

[43] Liu, Y., Zhou, Y., and Lu, J. Exploring the relationship between air pollution and meteorological conditions in China under environmental governance. *Scientific Reports*, 10(1):1-11, 2020.

[44] Wang, J., and Christopher, S. A. Intercomparison between satellite-derived aerosol optical thickness and $PM_{2.5}$ mass: Implications for air quality studies, *Geophysical Research Letters*, 30(21):2095, 2003.

[45] Koelemeijer, R., Homan, C., and Matthijsen, J. Comparison of spatial and temporal variations of aerosol optical thickness and particulate matter over Europe. *Atmospheric Environment*, 40:5304-5315, 2006.

[46] Liu, Y., Franklin, M., and Koutrakis P. Using aerosol optical thickness to predict ground-level $PM_{2.5}$ concentrations in the St. Louis area: A comparison between MISR and MODIS. *Remote Sensing of Environment*, 107(1-2):33-44, 2006.

[47] Kumar, N., Chu, A., and Foster, A. An empirical relationship between $PM_{2.5}$ and aerosol optical depth in Delhi metropolitan. *Atmospheric Environment*, 41:4492-4503, 2007.